Proceedings of the 32nd European Safety and Reliability Conference (ESREL 2022)
Edited by Maria Chiara Leva, Edoardo Patelli, Luca Podofillini, and Simon Wilson
 Published by Research Publishing, Singapore.
doi: 10.3850/978-981-18-5183-4_R04-03-475-cd

High-pressure jet and cylindrical obstacles in series: a CFD study

Giovanni Romano

Romano Safety Management S.t.P., Via Saore 25, Osio Sotto, 24046 Bergamo, Italy. E-mail: giovanni.romano@rsmstp.it

Dipartimento di Chimica, Materiali ed Ingegneria Chimica "Giulio Natta", Politecnico di Milano, Via Mancinelli 7, 20131 Milano, Italy.

Paolo Tombini

Romano Safety Management S.t.P., Via Saore 25, Osio Sotto, 24046 Bergamo, Italy. E-mail: paolo.tombini@rsmstp.it

Fabio Ferrario

Dipartimento di Chimica, Materiali ed Ingegneria Chimica "Giulio Natta", Politecnico di Milano, Via Mancinelli 7, 20131 Milano, Italy. E-mail: fabio.ferrario@polimi.it

Anna Mormile

Romano Safety Management S.t.P., Via Saore 25, Osio Sotto, 24046 Bergamo, Italy. E-mail: anna.mormile@rsmstp.it

Valentina Busini

Dipartimento di Chimica, Materiali ed Ingegneria Chimica "Giulio Natta", Politecnico di Milano, Via Mancinelli 7, 20131 Milano, Italy. E-mail: valentina.busini@polimi.it

This research focuses on the analysis of interactions between a high-pressure flammable gaseous jet and obstacles of varying shapes, dimensions, and numbers. Specifically, the studied obstacles are horizontal and vertical cylinders positioned in series. The presence of obstacles that can change the shape and maximum axial extension of the free jet is of particular interest when it comes to industrial and process safety, since, in the case of an incidental event, consequences are directly proportional to the axial extension of the flammable mixture. Nevertheless, the modelling of such consequences is not easy since models like gaussian or integral ones can not consider the presence of obstacles with satisfying outcomes. Consequentially, the usage of Computational Fluid Dynamic models is needed, although it will require a noticeable amount of time and energy to utilize them. It is necessary to find the ideal approach to reach rigorous and precise results that can meet industrial needs, with the objective to define the limits of how much the incidental scenario can be simplified without losing its significance.
Through the software ANSYS®, the task of this work is to analyse various configurations of the horizontal and vertical cylinders positioned in a series arrangement, a process with which we aim to identify the geometrical parameters that manage to modify the maximum axial extension of the lower flammable limit of high-pressure gaseous jets.

Keywords: natural gas, flammable jet, high-pressure release, jet impingement, cylindrical obstacles influence, Computational Fluid Dynamic.

1. Introduction

Among the most common incidental scenarios, high-pressure jets of gaseous substances have become particularly relevant in process industry (C. Colombini and V. Busini (2019)). Numerous studies of jet and obstacle interactions have been carried out, aiming to identify how the interaction with a single obstacle and, subsequentially, multiple obstacles changes the axial extension of the free jet. A free jet is defined as a jet that has no interactions with the environment in which it is released. The concentration gradient of the jet, be it subsonic or supersonic, will change along the axial and radial component of the jet, due to turbulence and air entrainment (C. Colombini (2020)). Ground-jet interaction are another fundamental aspect to consider: if the height of release of the jet is below a very specific height, the flammable mixture will interact with the ground, increasing its maximum extension, if compared to a free jet with no ground interaction (C. Colombini *et al.* (2020)). The following equation for the computation of the critical height is valid for methane releases:

$$ME = ME_{FJ} \cdot \left(3{,}89 - 0{,}22 \cdot \frac{h}{D_{ps}}\right) \quad (1)$$

ME is the maximum extent of the LFL of a generic jet, ME_{FJ} is the maximum extent of the free jet, h is the release height and D_{ps} is Birch's equivalent diameter.

2. Materials and methods: Birch's equivalent diameter

This work focuses on the gaseous release of methane (see Table 1) as a consequence of an incidental event. Birch's approach was used, which entails the introduction of a pseudo-diameter as the point of release to simulate the fully expanded jet (E. Franquet *et al.* (2015)). The pseudo-diameter (D_{ps}) defines a surface in front of the storage tank; such a surface is traversed by the same mass flow that exits from the orifice created by the incidental event. Through this approach, the equivalent diameter equation becomes the following (A. D. Birch *et al.* (1984)):

$$\frac{{D_{ps}}^2}{D^2} = C_d \cdot \frac{P_1}{P_3} \cdot \left(\frac{2}{\gamma + 1}\right)^{\frac{\gamma+1}{2\cdot(\gamma-1)}} \cdot \sqrt{\frac{T_3}{T_1}} \quad (2)$$

All CFD simulations were performed by using version 19.1 of ANSYS®. Each simulation was set up through the suite ANSYS® Workbench, which works as a user interface for the management of all the necessary modules. Three release conditions for the methane gas were studied, with variations of the incidental orifice size, storage pressure (see Table 1), and height of release (see Table 2):

Table 1. Release conditions of methane.

	Set1	Set 2	Set 3
Diameter of the orifice (mm)	25,4	25,4	50,8
Storage pressure (bar)	65	130	65
Equivalent diameter (mm)	146	206	292
Mass Flow (kg/s)	5,2	10,4	20,7

Thermophysical data of natural gas were taken from National Institute of Standards and Technology. Environment conditions were set up as P=1 atm and T=300 K.

2.1. Geometry

The geometry was constructed with ANSYS® Design Modeler. The data depends on the orientation and configuration of obstacles, which also influences the release height of the methane jet, as shown in Table 2:

Table 2. Geometry and release height.

	Diameter (m)	Height-Width (m)	Release height (m)
Horizontal cylinder	2	7	1,5
Horizontal cylinder	3	7	2
Vertical cylinder	2	7	4

As shown in Figure 1, five Body Lines, named Core, Far 1, Far 2, Far 3 e Far 4, were used to generate the mesh with the ANSYS® Meshing module.

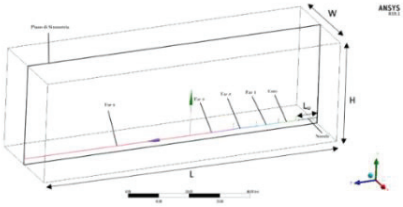

Fig. 1. Geometry of the domain.

Obstacle geometric data is listed in Table 3 and in Figure 2 and 3:

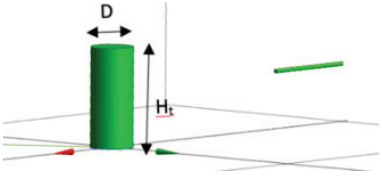

Fig. 2. Geometry of a vertical tank.

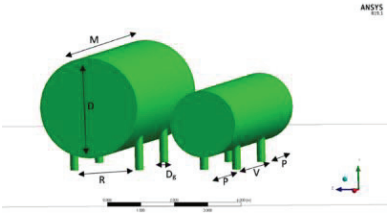

Fig. 3. Geometry of horizontal tanks: height from the ground = 0,5m.

Table 3. Horizontal tanks dimensions.

D (m)	D_g (m)	R (m)	P (m)	V (m)
2	0,25	1	2	3
3	0,25	2	2	3

In all simulations, the first obstacle is positioned in the halfway point of the maximum extent of the free jet. Symmetrical geometry is used, allowing for the simulation of only half of the domain.

2.2. Mesh

The construction of the mesh was conducted with ANSYS® Meshing. To limit computational resource spending, the mesh was modelled to be denser in proximity to the nozzle; furthermore, an independence test was performed, as such the listed parameters in Table 4 were used:

Table 4. Characteristic parameters of the mesh.

	Length (m)	Cell dimension (m)	Growth rate (m)
Nozzle wall	-	0,030	1,200
Methane inlet surface	-	0,015	1,200
Core	6	0,015	1,075
Far 1	8	0,022	1,100
Far 2	8	0,030	1,150
Far 3	10	0,090	1,175
Far 4	66	0,180	1,200
Obstacle surface	-	0,015	1,200

2.3. Setup

To define the boundary conditions of the model, ANSYS® CFX-Pre was used. In this phase, boundary conditions and solver settings were setup. Boundary conditions are summarized in Table 5, which remain constant between all simulations, except for the flow rates (Table 1).

Table 5. Boundary conditions.

Wind inlet	Velocity (m/s)	Temperature (K)
Back Side	V_x= 0 V_y= 0 V_z= Power law	T= 300
Left side	V_x= 1E-09 V_y= 0 V_z= Power law	T= 300
Top Side	V_x= 0 V_y= 0 V_z= Power law	T= 300
Walls	Boundary conditions	Roughness (m)
Ground	No slip	0,01
Nozzle	No slip	Smooth wall
Tank	No slip	0,001

Velocity along the z axis is given by the following power law:

$$v(z) = v_{10} \cdot \left(\frac{z}{10}\right)^{\beta} \quad (3)$$

Where v_{10}=5 m/s is the wind velocity measured at a height of 10 m and β=0,25 is an exponential factor that considers the atmospheric stability of the environment and characteristics of the ground. In Table 6, solver settings are listed.

Table 6. Solver settings.

Parameter	Solver settings
Turbulence model	k-ω Shear Stress Transport
Heat Transfer model	Total Energy
Turbolence numerics	High Resolution
Physical timescale	0,1 s
Convergence criteria	RSM = 0,000001

2.4. Solution

To solve transport equations, ANSYS® CFX-Solver was used. Convergence of the solution was judged by the following parameters: momentum-mass and imbalance.

2.5. Results

Results were processed with ANSYS® CFD-Post. Result evaluation is mainly based on two parameters: the extension of the lower flammable limit and eddy generation. The former parameter is used to judge the maximum extension (ME) of the flammable jet and eventual jet-ground interactions. The presence of eddies serves to evaluate the influence of obstacles: eddy generation behind the obstacle brings further dilution of the flammable gas due to the strong mixing introduced, lowering methane concentrations below the lower flammable limit; thus, reducing the maximum extend of the jet.

3. Results and discussion

On the basis of previous research (G. Romano, P. Tombini *et al.* (2021)), this work was focused on cylindric tanks, with a vertical and horizontal orientation. Each simulation varies in the release set, obstacle diameter (D), and distance between the centre of obstacles (s).

3.1. Studied scenarios

Each case listed in Table 7 and Table 8 was simulated with the structure listed in Table 9, so that each case had 7 simulations, for a grand total of 77 cases simulated for this work:

Table 7. Cases performed for Vertical cylinders.

Cases	Diameter D [m]	Release set
a	2	Set 1
b	3	Set 1
c	2	Set 2
d	2	Set 3
e	3	Set 3

Table 8. Cases performed for horizontal cylinders

Cases	Diameter D [m]	Release set
a	2	Set 1
b	3	Set 1
c	2	Set 2
d	3	Set 2
e	2	Set 3
f	3	Set 3

Table 9. Structure of each case related to Table 7 and Table 8.

Ref	s/D [-]
FJ	n.a.
0	0
1	2
2	2,5
3	3
4	4
5	5

3.2. Ground influence analysis

Ground influence is one of the fundamental aspects must be thoroughly analysed to have a complete comprehension on how the maximum extent of a jet is affected by the environment. Eq. (1) estimates whether the jet will interact with the ground as the height of release varies. From this same equation, a value of $H/D_{ps}<13$ guarantees that the free jet will interact with the ground. Since D_{ps} varies with the set, the previously

mentioned ratio depends on a critical height of release for each set:

Table 10. Boundary conditions.

Set number	Critical Height H_c (m)
Set 1	1,9
Set 2	2,7
Set 3	3,8

If the release height is lower than the critical height, free jet-ground interactions are guaranteed; on the other hand, if the release height is higher than the critical height, free jet-ground interactions are unable to occur. All cases that involve a vertical obstacle will lack free jet-ground interactions, while the free jet of horizontal obstacles mostly interacts with the terrain; therefore, in the latter case the *ME* is mainly influenced by the terrain, in fact the relation for terrain influence depicted in Figure 5 well fits the data.

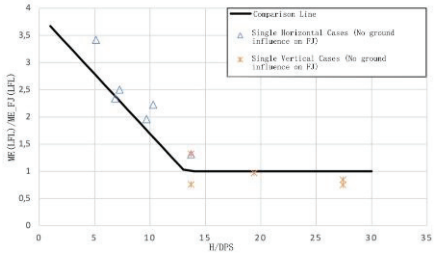

Fig. 5. Value of ME as H/D_{ps} varies with a single obstacle.

3.2.1. Cases with a single obstacle

For horizontal cases, as seen in Figure 5, ground influence was found to be a very influential factor for the extension of the jet, since most of the free jet simulated for each set of cases has free jet-ground interaction. In half of the cases, the presence of the single obstacle is, for the most part, significant in the variation of the maximum extent of the jet (with percentual variations to the ME_{fj} lower than 10%). For case *c*, case *d* and case *e*, the presence of the obstacle is negligible due to its ME being the same as ME_{FJ}. On the other hand, case *a*, case *b* and case *f* display different results from the previous three, showcasing percentual variations that exceed well beyond the 10% limit.

For vertical cases, depicted with plotted point at H/D_{ps} =13 in Figure 5, ground influence was found to be not as important for the extension of the jet, except for case *e*, since all free jet simulated for each set of cases has no free jet-ground interaction. On account of the lack of ground influence, the single vertical obstacle limits the extension of the jet, leading to results that reduce the maximum extent to percentual variations below 10% for all cases, except case *e*, because of the interaction of the jet with the obstacle, it manages to lower the axial height of the jet and allow jet-ground interactions, elongating the maximum extent of the jet by 31%. Results are shown in Table 11:

Table 11. Results of the ME/ME_{FJ} for single obstacles.

Cases	Horizontal cylinders	Vertical cylinders
Case a	1,15	0,84
Case b	-	0,74
Case c	0,97	0,96
Case d	1,01	0,75
Case e	1,04	1,31
Case f	0,82	-

3.2.2. Cases with tandem obstacles

Maximum extent variations of the jet are mostly due to two phenomena, as shown if Figure 6: jet dilution (Focus 1) and jet-ground detachment (Focus 2).

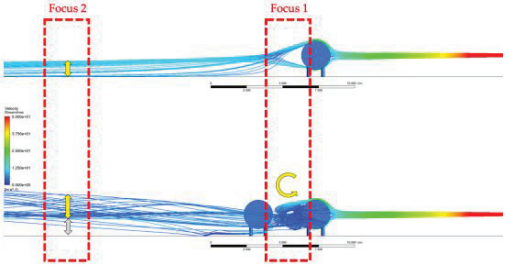

Fig. 6. Velocity streamlines of the jet.

In regard to the dilution of the jet, when it hits the first obstacle in the presence of a second obstacle, a considerable quantity of eddies will form behind the first tank (Focus 1), trapping the jet and

leading to further mixing with the surrounding air. Jet-ground detachment will happen when the jet goes beyond the second tank, leading the increase of the height of the axis of the jet (Focus 2), limiting jet-ground interactions, promoting the shortening of the maximum extent of the jet. Simulation results of horizontal tanks with tandem arrangement, shown in Figure 7, at a certain value of s/D, for all cases, there is a decrease in maximum extend, as the length of the jet returns to similar values that were found in the single obstacle study (s/D=0). All cases, except for case *f*, have ME changes caused by the presence of the second obstacle with a percentual variation to the ME_{single} over 10%. The lowest value achieved is found in case *c,* which display jet-ground detachment behaviour (Focus 2, D=2 m and set 2) with ME_{tandem}/ME_{single} =0,7 for a distance between tanks of 4 m.

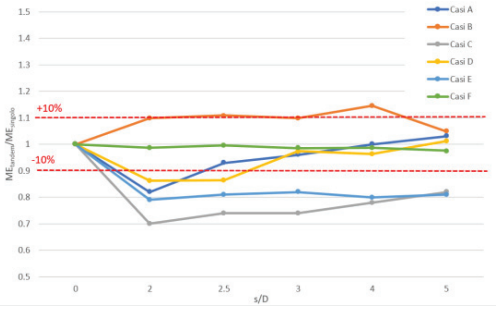

Fig. 7. ME/ME_{single} as s/D varies for horizontal tanks.

From this analysis, variations found as a consequence of second obstacle-jet interactions lead to a shortening of the maximum extent of the jet, showcasing a smaller role played by the influence of the ground.

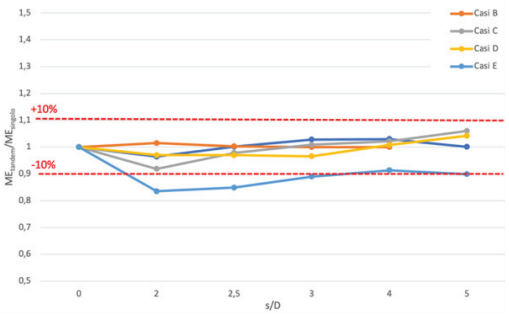

Fig. 8. ME/ME_{single} as s/D varies for vertical tanks.

In the results of the vertical tanks with tandem arrangement shown in Figure 8, most cases demonstrate that the presence of the second obstacle leads to the decrease of the maximum extent of the jet, or at the very least, it will have no influence in the maximum extent of the jet. As predicted by Eq.(1) and described by Figure 5, all changes to the jet length are due to the influence of the obstacles, with little influence from the ground, except for specific cases. For lower values of s/D, the presence of the second obstacle will shorten the maximum extent of the jet. This behaviour is demonstrated to be caused by the generation of a high number of eddies behind the first obstacle, as it is portrayed by Figure 9. These eddies will then promote the dilution of the gas. As the relative distance s/D between the first and second obstacle increases, the influence of the second obstacle will be less prominent, as eddy formation decreases with it.

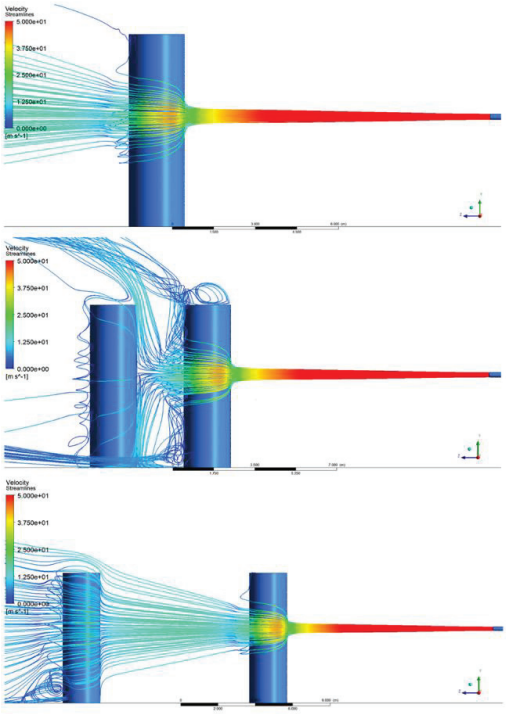

Fig. 9. Eddy formation between obstacles.

Nevertheless, although the jet in no longer influenced by the dilution process of the eddy, the

roughness of the surface of the second obstacle, will allow for the Coanda effect (B. D. Giles (1976)) to take place, leading to an increase in length of the jet beyond the second obstacle. After a certain value of s/D, the effect previously described will also become irrelevant, returning the length of the maximum extent of the jet to the one found in the simulation with a single obstacle. It is possible to discriminate a certain pattern in the behaviour of vertical cylindrical obstacles, where the jet will decrease in length and as the s/D increases, its length will return to the one that was found in the simulation with the free jet.

Three zones can be described: a first "turbulent zone" in which the second obstacle leads to an increase in eddy generation behind the first obstacle, decreasing the length of the maximum extent of the jet; a "dragging zone" where the surface of the second obstacle leads to the "dragging" of the jet due to the Coanda effect and the lack of eddies allow the lengthening of the maximum extent of the jet beyond the second obstacle; a final "neutral zone", where the second obstacle does not have any effect in the maximum extent of the jet, behaving as if only the first obstacle has any influence on it.

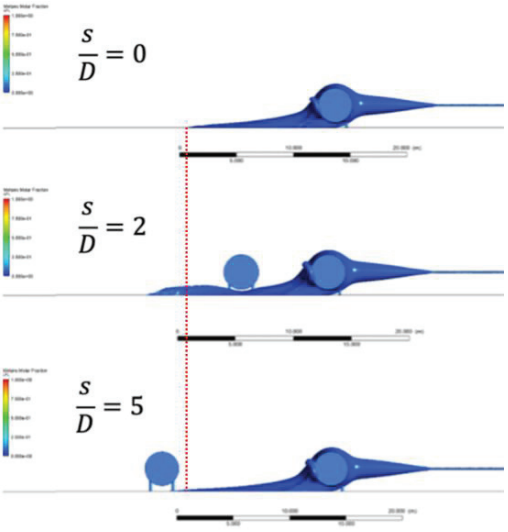

Fig. 11. Comparison between jets with one and two obstacles with varying distances.

As shown in Figure 11, this leads to the regression of the maximum extension of the jet to what was recorded for the single obstacle simulation, as can be clearly seen in the results from Figure 7 and Figure 8. This phenomena manifests in different values of s/D.

4. Conclusions

The following conclusions are separated for single obstacle cases and tandem obstacles cases

4.1. Cases with a single obstacle

If it is not possible to exclude terrain interaction with the free jet, the presence of a single obstacle will be mostly influential, resulting with maximum extent values which are roughly the same ones for the free jet. The previous statement is not generalizable due to case *a* and case *f* for horizontal tanks, which show a lengthening and shortening of the maximum extent respectively, when compared to their free jets. These phenomena occur due to a change in direction of the jet towards the ground by the obstacle in case *a*, while the jet is forced to detach from the ground by the obstacle in the case *f*. If it is possible to exclude terrain interaction with the free jet; the presence of the single obstacle will lead to further dilution of the jet, consequentially, diminishing the maximum extent of the jet. Nevertheless, this statement is not generalizable due to case *b* for horizontal cylinders and case *e* for vertical cylinders, that showcase a lengthening of the jet due to the jet interaction with the ground after surpassing the first obstacle. Thus, when an obstacle is present, even when $H/D_{ps}>13$ (Eq. (1)), it is not enough to guarantee that no ground interaction will occur.

4.2. Cases with two obstacles

Minimum distances between tanks follow standardized tank guidelines. The presence of the second obstacle has a limited effect in the extension of the jet, or at the very least, it will lead to the shortening of its length. Therefore, the presence of the second obstacle will not have a strong influence from the point of view of industrial risk management.

This behaviour, for both horizontal and vertical tanks, is caused by the dilution of the jet by the promotion of eddy generation by the second obstacle. For horizontal cases, terrain interaction will be limited by this effect, while for vertical cases, terrain interaction will almost never occur,

while still inducing a reduction in the jet length. These statements are not generalizable due to the case *b* for horizontal cylinders which lengthen the jet maximum extent, since the second obstacle forces further jet-terrain interaction. In horizontal cases where the jet was shortened when compared to the single obstacle, another phenomenon was observed: in case *c*, the impingement of the jet with the obstacle forces the detachment of the jet from the ground, limiting ground-jet interactions. It was not possible to find a valid model that allows the prediction of the jet behaviour beyond its impingement with the second obstacle, whether or not terrain detachment will occur. This is because of a limited number of cases where the phenomena can be observed.

5. Future prospects

Four areas of interest were identified to develop pertaining to the topic of jet impinging with multiple obstacles. Firstly, further elaboration on the way the jet behaves as the first obstacle changes position, removing the condition of it being positioned at the halfway point of the maximum extent of the free jet, to verify the conclusions reached in this study remain valid at different distances. Secondly, for horizontal obstacles the position of the first obstacle and release set must be changed to compute a suitable equation that allows the prediction of when the detachment of the jet from the ground occurs, leading to a shortening of the maximum extent and when the jet is pushed to the ground, leading to a lengthening of the maximum extent (Figure 6). Thirdly, for the height of release, in the case of horizontal cylinders, researching whether the positioning of the nozzle over or under the median of the obstacle could have any effect on the jet. The expected behaviour is that if the nozzle is positioned such that the axis of the jet is over the median of the tank, the latter will work as a ramp for the jet. Lastly, further investigation in the conditions at which the free jet is released at a height higher than the critical height (1) but the jet, due to jet-obstacle interaction, is brought to the ground, leading to the lengthening of the jet, nonetheless. As such, positioning the jet at a height that is equals or above the critical height is not enough to guarantee a lack of jet-ground interaction with the presence of an obstacle. Simulations with increasing values of release height must be carried out, to estimate a new critical height that guarantees no interaction with the ground, even when an obstacle is present.

6. References

C. Colombini and V. Busini (2019). *Obstacle influence on high-pressure jets based on computational fluid dynamics simulations*. Chemical Engineering Transactions.

C. Colombini, L. Carlini, R. Rota and V. Busini (2020). *Ground interaction on high-pressure jets: Effect on different substances.* Chemical Engineering Transactions.

C. Colombini, A. Martani, R. Rota and V. Busini (2020). *Ground influence on high-pressure methane jets: practical tools for risk assessment*. Journal of Loss Prevention in the Process Industries.

E. Franquet, V. Perrier, S. Gibout and B. Pascal (2015). *Free underexpanded jets in a quiescent medium: A Review*. Progress in Aerospace Sciences.

A. D. Birch, D. R. Brown, M. G. Dodson and F. Swaeld (1984). *The structure and concentration decay of high pressure jets of natural gas*. Combustion Science and Technology.

G. Romano, P. Tombini, P. Blas and V. Busini (2021). *Multi-obstacles influence on High-Pressure Methane Jets*. Research Publishing.

B. D. Giles (1976). Fluidics, *the Coanda Effect, and Some Orographic Winds*. University of Birmingham.